Combustion and Flame 162 (2015) 1095–1103

Contents lists available at ScienceDirect

Combustion and Flame

journal homepage: www.elsevier.com/locate/combustflame

Flame necking-in and instability characterization in small and medium pool fires with different lip heights

Longhua Hu [a,*], Junjun Hu [a], John L. de Ris [b]

[a] State Key Laboratory of Fire Science, University of Science and Technology of China, Hefei, Anhui 230026, China
[b] FM Global, Research Division, Norwood, MA 02062, USA

ARTICLE INFO

Article history:
Received 24 April 2014
Received in revised form 1 October 2014
Accepted 1 October 2014
Available online 28 October 2014

Keywords:
Flame necking-in depth (velocity)
Necking-in uprising height (velocity)
Rayleigh–Taylor instability
Puffing instability
Frequency
Characteristic life-time

ABSTRACT

Flame necking-in is a fundamental behavior at the base of diffusive pool fires caused by the entrained flow approaching the flame induced by buoyancy (density difference), which is also the major generation source of flame periodic oscillatory instability. However, measurements have not been previously reported for the evolution of the flame necking-in dynamic characteristics and how they relate to flame instability behaviors. This paper quantifies the flame necking-in dynamics and instability motions in 0.04–0.25 m diameter ethanol pool fires with different lip heights (0.3–2 cm). Based on direct time-sequence analysis on flame photographs, the necking-in characteristic maximum depth ($\mathcal{D}_{max}$), average necking-in velocity ($U_{necking\text{-}in}$), maximum uprising height ($\mathcal{H}_{max}$), average uprising velocity ($U_{uprising}$), as well as the vortices shedding instability frequency (f) and characteristic vortices formation lift-time (τ) are quantified to find their evolutions with pool size and lip height along with their associated dominant instability motions. Three different flame instability motions are identified: short life Rayleigh–Taylor (*R–T*) instability, extended *R–T* instability and puffing instability. The dominant instability motion is found to transit from extended *R–T* instability to puffing instability with increase in pool size or lip height. The pumping capacity of large-scale vortices formation (which could be quantified by $\mathcal{D}_{max}$, $\mathcal{H}_{max}$, $U_{necking\text{-}in}$, $U_{uprising}$) is primarily associated with the extended *R–T* instability frequency. The frequency (f) of the necking-in extended *R–T* instability is found to be greater than the puffing frequency. The puffing frequency increases slightly with lip height and decreases with pool diameter, D, following the well-known pool fire square root law ($f \sim D^{-1/2}$, or non-dimensionally $St \sim Fr^{-1/2}$). Meanwhile the frequency (f) for Extended *R–T* instability is found to be well correlated by $f_{R-T,extended} \sim (\ell_f g^2/\dot{Q})^{1/3}$. The characteristic life-times (τ) of the extended *R–T* instabilities increase with pool diameter while remaining smaller than the puffing life-times that scale by $\tau \sim D^{1/2}$.

1. Introduction

Flame necking-in is a fundamental phenomenon at the base of diffusive pool fires. This behavior is caused by the entrained flow approaching the flame induced by buoyancy (density difference), which drives the flame instabilities (periodic oscillatory). There were several discussions on flame instability motions in the literatures (as reviewed briefly below) [1–12]; however no direct measurements have been made of the evolution of the flame necking-in dynamic characteristics and how these two behaviors (necking-in, instability) are related.

The periodic oscillatory motion close to the base of a buoyant diffusion flame is often described as puffing, and its characteristic frequency is inversely proportional to the square root of source diameters [1–6]. Hamins et al. [5] have demonstrated that puffing behavior can also happen even in the absence of combustion (isothermal helium plumes). Weckman and Sobiesiak [2] have studied the visible fire structure as well as pulsation frequency by varying the boundary conditions on a burner. Cetegen and Kasper [7] have shown that non-reacting buoyant plumes have similar frequency characteristics but with different frequency scaling, because combustion sustains the driving density difference while in non-reacting buoyancy plumes density difference decreases because of cool air entrainment from surroundings. Cetegen and Dong [8] have shown that for buoyant diffusion flames, both sinuous mode and varicose mode can occur; but for non-reacting buoyant plume, only varicose mode occurs. They also show that the two modes have different frequencies.

In fact, different mechanisms have been proposed to explain the nature of such instabilities. Cetegen and Kasper [7] attributed

* Corresponding author. Fax: +86 551 63601669.
E-mail address: hlh@ustc.edu.cn (L. Hu).

http://dx.doi.org/10.1016/j.combustflame.2014.10.001
0010-2180/

puffing to Rayleigh–Taylor (*R–T*) instability. Ghoniem et al. [9] attributed it to both *R–T* instability and Kelvin–Helmholtz (*K–H*) instability. Coats [10] showed that *K–H* instability is the cause in momentum-dominated flows of which velocity differences dominate. But the density difference still exists and cannot be ignored in the momentum-dominated flows. de Ris [11] proposed a fluid vorticity analysis for the *R–T* instability in buoyant diffusion flames. Cetegen [4,12] showed that the puffing mechanism comes from the close coupling of the base with shedding vortices.

Experiments are performed in this work for small and medium size pool fires having different lip heights, so as to quantify the flame necking-in dynamic characteristics and clarify whether the periodic shedding of vortices from the base is purely a simple *R–T* instability or a puffing instability or coupling of them by examining the dynamics of their necking-in characteristics, shedding frequencies and vortex life-times as function of pool diameter and lip height. The characteristic necking-in structure dimensions ($\mathcal{D}_{max}$, $\mathcal{H}_{max}$) and macroscopic velocities ($U_{necking\text{-}in}$, $U_{uprising}$) are quantified by directly analyzing time-sequence flame photographs. The characteristic necking-in vortex shedding frequencies and life-times are then discussed and understood more deeply in terms of the different instability motions.

2. Experimental setup

Experiments were carried out in a quiescent air and under steady state conditions. Care was taken to eliminate all sources of external vorticity that might disturb the flames. Circular burners of diameters, 0.04, 0.06, 0.08, 0.10, 0.15, 0.20, 0.25 m used in the experiments, cover both the laminar and turbulent flame flow regimes as well as the transition between them. The burners were mounted a considerable distance above the laboratory floor to minimize drawing in any external vorticity that might disturb the flame. Figure 1 shows the 8 cm high circular burners having 2 mm thick stainless steel walls. A stainless steel net was placed inside the pools 5 cm below the top rim to hold glass beads (5 mm diameter). The depth of glass beads was changed for different lip heights to maintain a 1.0 cm distance from the top surface of the glass beads to the fuel surface as shown in Fig. 1. The glass beads were used to reduce the effects of distillation and convective currents either driven thermally or from the bottom (hole) fuel supply [13]. The fuel surface level was controlled by the method used in [14], similar to that of Rasbash et al. [15]. It consists of three fuel storages. The fuel surface in the second storage is kept at the same level with that designed for the pool fire. The fuel is supplied from the first storage into the second storage, with excess fuel (above the fuel surface level) flowing to the third storage. Three typical lip heights were considered, 0.3 cm, 1.0 cm, and 2.0 cm. The 0.3 cm lip height was used rather than zero lip height because the surface tension effect for zero lip heights tends to increase the original size of base. Diameter of 8 cm and 10 cm (as these two diameters are included in the critical transitional regime for different instability motions) with lip heights of 0.4 cm, 0.6 cm and 0.8 cm were also additionally employed to investigate the sensitivities of different instability modes to diameter–lip boundary conditions. The mass regression rate was measured by an electronic balance [14] with resolution of 0.1g and with sampling interval of 1.0 s. The heat release rate was then calculated based on the mass regression rate measured and the heat of combustion of the fuel.

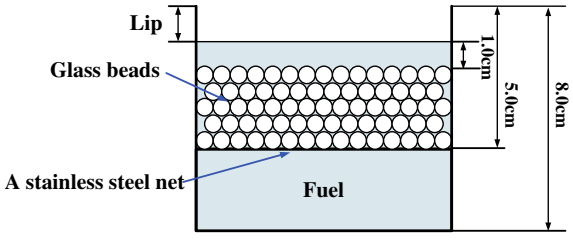

Fig. 1. Design of pool fire burner.

Two CCD cameras were used to record the geometrical and frequency information of the flame: one at 25 fps with 3,000,000 pixels and the other at 60 fps with 350,000 pixels, to eliminate uncertainties caused in direct time-sequence analysis on the recorded flame photographs, especially for the frequencies. The faster one was necessary for the 4 cm diameter pool fires with 1 cm or 2 cm lip heights which had relatively higher flame oscillation frequencies. The results from the two cameras were the same for all the other fires. Black masking paper was put on the wall behind the fires to prevent reflections from the wall influencing the flames and recorded images. The experiments were repeated three times for each pool size and each lip height, showing good repeatability.

3. Result and discussion

3.1. Flame motion and necking-in macroscopic structure

Figure 2(a) and (b) shows typical flame motions (time interval between frames is 1/25 s): Rayleigh Taylor (*R–T*) instability and puffing instability, which are observed to be entirely different. *R–T* instability occurs within the flame volume and should be independent of the base. Consider a vortex tube (shown schematically in Fig. 2c) [11], having circulation $\Gamma(t)$ around a closed path $C(t)$ surrounding the vortex tube and cross-sectional area $A(t)$. The vorticity going through the area $A(t)$ is $\int_{A(t)} \vec{\omega}\cdot\mathbf{n}dA$. The circulation $\Gamma(t)$ can be expressed by Stokes Theorem:

$$\Gamma(t) = \oint_{C(t)} \vec{v}\cdot d\vec{l} = \int_{A(t)} \vec{\omega}\cdot\mathbf{n}dA \tag{1}$$

Its rate of change is

$$d\Gamma(t)/dt = \oint_{C(t)} (\mathrm{D}\vec{v}/\mathrm{D}t)\cdot d\vec{l} = \int_{A(t)} \nabla\times(\mathrm{D}\vec{v}/\mathrm{D}t)\cdot\mathbf{n}dA + \oint_{C(t)} \vec{v}\cdot(d\vec{l}\cdot\nabla)\vec{v} \tag{2}$$

The second integral is zero because goes around a closed path, then Eq. (2) becomes

$$d\Gamma(t)/dt = \oint_{C(t)} (\mathrm{D}\vec{v}/\mathrm{D}t)\cdot d\vec{l} = \int_{A(t)} \nabla\times(\mathrm{D}\vec{v}/\mathrm{D}t)\cdot\mathbf{n}dA \tag{3}$$

Considering the momentum equation for buoyant diffusion flames,

$$\rho\frac{\mathrm{D}\vec{v}}{\mathrm{D}t} = \rho\left[\frac{\partial\vec{v}}{\partial t} + (\vec{v}\cdot\nabla)\vec{v}\right] = -\nabla p + \rho\mathbf{g} + \Phi \tag{4}$$

where p is the total pressure, $\mathbf{g}$ is the downward acceleration and Φ is the viscous stress tensor. Taking the curl of Eq. (4) one has

$$\rho\nabla\times\frac{\mathrm{D}\vec{v}}{\mathrm{D}t} = \rho\nabla\times\left[\frac{\partial\vec{v}}{\partial t} + (\vec{v}\cdot\nabla)\vec{v}\right] = \nabla\rho\times\left(\mathbf{g} - \frac{\mathrm{D}\vec{v}}{\mathrm{D}t}\right) + \nabla\times\Phi \tag{5}$$

The first term on the RHS (Right-Hand-Side) is the baroclinic generation of vorticity.

Combining Eqs. (3) and (5) results in